TWO DIMENSIONAL PHOTONIC CRYSTALS WITH DIFFERENT SYMMETRIES FOR WAVEGUIDES AND RESONANT CAVITIES APPLICATIONS

Dana Georgeta POPESCU[1]

In this paper we investigate the properties of two-dimensional photonic crystals (2D PhCs) with both hexagonal and square symmetry for applications in optoelectronics and telecommunication. An efficient way of manipulating the light is to make use of the defects introduced within the periodic structure, which consequently break the symmetry of the crystal, resulting in linear waveguides or resonant cavities. We calculate using finite-difference time-domain and finite-difference frequency-domain methods the properties associated with several kinds of defects, conveniently selected, performed in 2D PhCs with square and hexagonal symmetry.

Keywords: photonic crystal, waveguide, resonant cavities

1. Introduction

Photonic crystals (PhCs) are artificially fabricated periodic dielectric structures for controlling the propagation of light [1-3,13]. The existence of photonic band gaps (PBGs) plays a crucial role for the design of photonic integrated circuits. These optical materials can find various applications in the design of optoelectronic devices such as resonant cavities for optical light, optical logic gates, optical switches, beam splitters, demultiplexers, ring resonators [4-11]. By introducing certain defects within the PhC, localized modes can appear. If they sustain a radiation with well-defined frequency, the defect can further be used for guiding or amplification of light along the defect.

In this paper we investigate the properties of 2D PhCs. We have considered hexagonal and square symmetry in analyzing the features of these materials that can be used for applications in optoelectronics and telecommunication. We have studied the behavior of defects introduced in these periodical systems, especially focusing our attention over the ones created by the removal of a row of elements (W1) and resonant cavities. Thus, at well-defined frequencies supported by the defect, and subsequently calculated, the radiation field may be confined along the waveguide or inside the resonant cavity. We show how by tailoring the shape of the defect, and the lattice parameters, a broad frequency range may be covered and the efficiency of optical devices may be improved. All the calculations were performed using the finite-difference time-

[1]Ing., National Institute for Materials Physics, Atomistilor 105, Magurele-Bucharest, 077125, Romania, e-mail: dana.popescu@infim.ro

domain (FDTD) and finite-difference frequency-domain (FDFD) methods [2, 3, 9, 12].

2. FDTD method

The FDTD method is a direct discretization of Maxwell's differential equations, differential being replaced by finite differences [12,14-17]. It is used to solve a vast area of problems regarding electromagnetic waves, such as scattering, antenna analysis, wave propagation, electronic circuits, etc.

We can write the time-dependent Maxwell's curl equations for a linear isotropic material in a source-free region in the following form:

$$\frac{\partial \vec{H}}{\partial t} = -\frac{1}{\mu(\vec{r})}\nabla \times \vec{E} \tag{1}$$

$$\frac{\partial \vec{E}}{\partial t} = \frac{1}{\varepsilon(\vec{r})}\nabla \times \vec{H} - \frac{\sigma(\vec{r})}{\varepsilon(\vec{r})}\vec{E} \tag{2}$$

where $\vec{E}$ is the electric field intensity, $\vec{H}$ is the magnetic field intensity and $\varepsilon(\vec{r}), \mu(\vec{r}), \sigma(\vec{r})$ are the position dependent permittivity, permeability and conductivity of the material.

One can discretize in space and time Maxwell's equations by so called Yee-cell technique on a discrete 3D mesh. Figure 1 depicts the unit Yee cell of a 3D mesh. The (3)-(5) formulas constitute the discretization in space and time of Maxwell's equations on a discrete 3D mesh in a Cartesian *xyz* coordinate system [18-21], which indicate that values of the magnetic field intensity are taken with time shift as related to the electric field and its allow us to carry out the step by step computation of the electric field. Solution of the Maxwell's equations require information about the permittivity and permeability in computation nodes and the field distribution must be specified at least at one boundary so the computation could start. Also, the (3)-(5) formulas have similar counterparts for the magnetic field.

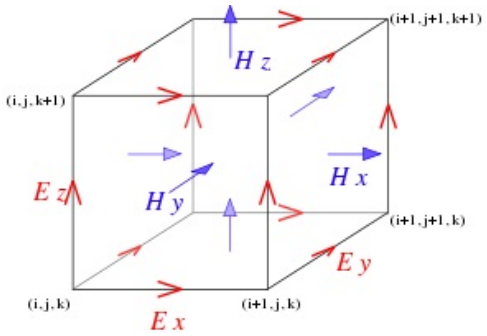

Fig. 1. The illustration of a standard Cartesian Yee cell.

$$E^{i+1}_{x(m,n,p)} = E^{i}_{x(m,n,p)} + \frac{c\Delta t}{\varepsilon_0 \varepsilon_r}\left(\frac{H^{i+1/2}_{z(m,n+1/2,p)} - H^{i+1/2}_{z(m,n-1/2,p)}}{\Delta y} - \frac{H^{i+1/2}_{y(m,n,p+1/2)} - H^{i+1/2}_{y(m,n,p-1/2)}}{\Delta z}\right) \quad (3)$$

$$E^{i+1}_{y(m,n,p)} = E^{i}_{y(m,n,p)} + \frac{c\Delta t}{\varepsilon_0 \varepsilon_r}\left(\frac{H^{i+1/2}_{x(m,n,p+1/2)} - H^{i+1/2}_{x(m,n,p-1/2)}}{\Delta z} - \frac{H^{i+1/2}_{z(m+1/2,n,p)} - H^{i+1/2}_{z(m-1/2,n,p)}}{\Delta x}\right) \quad (4)$$

$$E^{i+1}_{z(m,n,p)} = E^{i}_{z(m,n,p)} + \frac{c\Delta t}{\varepsilon_0 \varepsilon_r}\left(\frac{H^{i+1/2}_{y(m+1/2,n,p)} - H^{i+1/2}_{y(m-1/2,n,p)}}{\Delta x} - \frac{H^{i+1/2}_{x(m,n+1/2,p)} - H^{i+1/2}_{x(m,n-1/2,p)}}{\Delta y}\right) \quad (5)$$

In (3)-(5), c is the speed of light, ε_0 is the dielectric permittivity in vacuum, ε_r the relative permittivity of the medium, $E^{i}_{x,y,z}$ and $H^{i+1/2}_{x,y,z}$ are the electric and magnetic fields components in the Yee computational cell, defined as in Fig. 1.

For a fixed total number of time steps the computational time is proportional to the number of discretization points in the computational domain (FDTD algorithm is of order *N*).

Another technical point for FDTD method which should be mentioned is that for achieving convergence results the maximum mesh size should be at least 10% of the interested minimum wavelength [12]. To keep the stability of the method the time domain step should follow the Courant-Friedrichs-Levy condition [21-23]:

$$\Delta t \le \frac{1}{v\sqrt{\frac{1}{\Delta x^2} + \frac{1}{\Delta y^2} + \frac{1}{\Delta z^2}}} \quad (6)$$

where $\Delta x, \Delta y, \Delta z$ is the space domain step and v is the speed of light in the layout. Also we used the perfectly matched layer (PML) boundary condition [12] to keep the outgoing waves from being reflected back.

In order to preserve the interaction between neighboring crystal pillars the absorption in the PML's should increase quite gradually toward outside.

The FDTD method is one of the most popular numerical methods making no assumption about the direction of wave propagation or the time varying of the fields. There are no plane wave assumption, no slowly varying envelope

approximation and no modal expansions. It is capable of modeling the geometrical complexities and material in-homogeneities of realistic micro scale photonic and optoelectronic devices because of the rigorously enforces boundary conditions at material interfaces. So, a complete FDTD analysis of the electrodynamics of micro cavity lasers and resonators is computationally feasible because of the advanced state of computing power of workstations [24-28].

3. Results and discussion

Bound states in waveguides, and especially in waveguide bends, have been the subject of widespread theoretical and experimental investigation.

It was proved that bends always support bound states in constant cross-section quantum waveguides under the condition that the wave function vanishes on the boundary. Papers by Carini [22, 24] deal with calculating energies of single and multiple bound states in bent quantum waveguides and comparing them to results from microwave experiments.

Such research was stimulated by an interest in semiconductor device miniaturization and development of optical circuits. Since electronic transport properties through such quantum wires are influenced by the existence of localized states [17, 18], a good understanding of bound states in bends is relevant to building small-scale integrated circuits.

Our main goal was to understand and underline the basic mechanisms which drive the light propagation in waveguides based on 2D PhCs. More complex applications can be further designed, and the case of coupled optical cavities is presented.

The field of photonics is by now a fully mature one, in the last two decades significant progress being made in both theoretical aspects as well as experimental issues. On the other hand, still the widest used material for various applications concerning trapping the light in resonant cavities or its guiding in linear or bent waveguides remains Si. Our paper presents comparatively the way how Ge may be used as efficient alternative, since processing Ge surfaces is more practical than Si ones. Silicon by itself is cheaper than Ge, but as far as various heterostructures for microelectronics use are concerned, Ge can be more practical. At least in ultra-high vacuum conditions, it requires a lower cleaning temperature, which is prerequisite for its use as buffer layer for electronic circuits design [19-21,29]. Also, Ge provides a higher refraction index contrast.

We analyzed the most common waveguide, W1. The dispersion relations for the photonics bands were calculated in the (11) direction, corresponding to Γ-X direction for the square lattice and Γ-M direction for the hexagonal one along which the defect is oriented (see Fig. 2).

We considered the situation of a PhC designed by periodic cylinders of Si (ε_r=11.8) and Ge (ε_r=16), for structures having square and hexagonal symmetry,

varying the radius of the cylinders from 0.25*a* to 0.4*a*, with *a*, the lattice constant of our PhC.

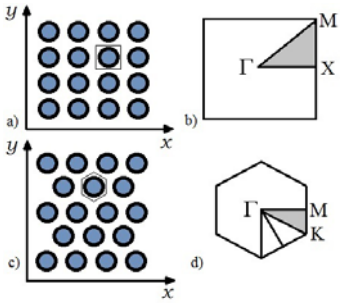

Fig. 2. The square lattice a) and the first Brillouin zone b); the triangular lattice c) and the first Brillouin zone d).

These relations for the PBG waveguides are calculated by solving Maxwell's equation in the frequency domain for a given dielectric configuration, using the MPB software [30]. A supercell with periodic boundary conditions is taken as the computational domain. The length of the cell corresponds to the periodicity of the dielectric in the direction of the guide, whereas the width was taken to be several lattice constants. The PhC simulated in this way contains parallel, evenly spaced waveguides.

In every case, the calculations are firstly performed on the un-defective structure, and the projected band-diagram is obtained for the pure crystal, containing no defects. Subsequently calculating the band system for the structure with an induced defect, and superimposing the two dispersion relations for the photonic bands, it is easy to identify which are the modes supported by the defect only.

Fig. 3 presents the dispersion lines for W1 waveguide designed in 2D PhCs with square symmetry, calculated along the Γ-X line, in order to capture the effects introduced by the defect.

Overlapping the bands of the crystal with no defect and the ones of the structure with linear waveguide, we observe that most of the features are common to both Si and Ge. The bands depicted in blue (□) are the bound states supported by the linear defect. This is ideally the case when a radiation field incident on the PhC having the frequency equal with the defect mode frequency can be guided without losses.

As we can see, there is no gap for both TE and TM modes. In the case of Si and Ge as well, there is only a gap for TM modes. The TM gaps are located approximately in the same frequency region for both Si-PhC and Ge-PhC. For Ge the first one (B1) in 0.18-0.33 and the second (B2) in 0.41-0.48, while for Si there are three TM gaps, 0.2-0.35 (B1), 0.41-0.48 (B2). In both cases, in the upper

frequency region (at ~0.63 for Ge and at ~0.82 for Si), there are some incomplete gaps which could guide only radiation with wave vector fulfilling the condition **k**~0 *i.e* around Γ point. Here, like in all the other projected band-diagrams along the paper the frequency is expressed in 2πc/a normalized units.

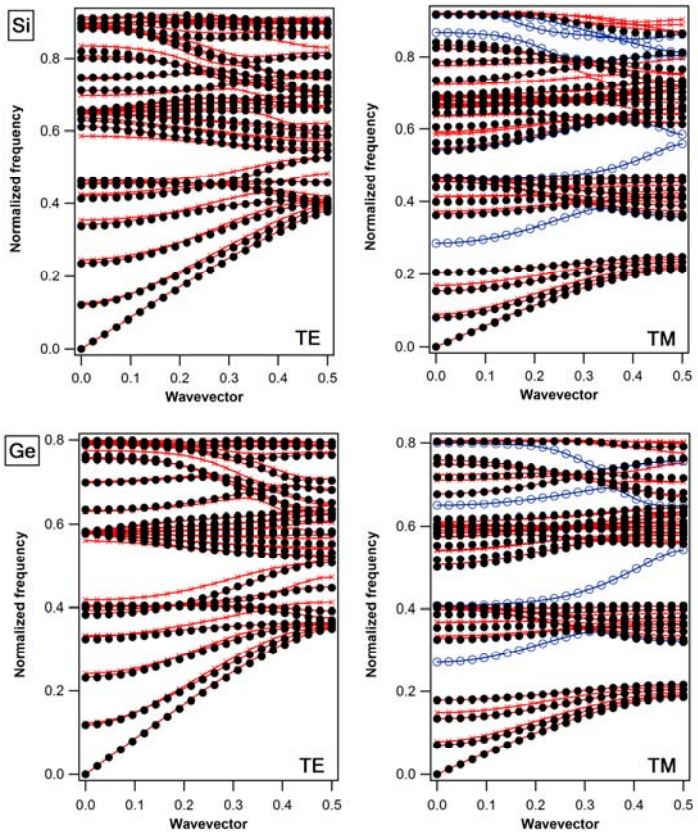

Fig. 3. Projected band-diagrams of W1 waveguide designed in a 2D PhC with square symmetry, using as materials Si and Ge and cylinder radius of r=0.25*a*. With black dots (●) are represented the bands of the pure crystal and with red lines (□), the ones of the defect. The blue lines (□), localized within the gap are associated with bound states supported by the defect.

For comparison, the structure based on a hexagonal lattice, with the radius of the cylinders having the same value (0.25*a*) is presented in Fig. 4. Again, the projected band-diagram was calculated only along the defect and the modes that lie within the stop gaps defined by the common regions of defective and perfect PhC are depicted in blue(□).

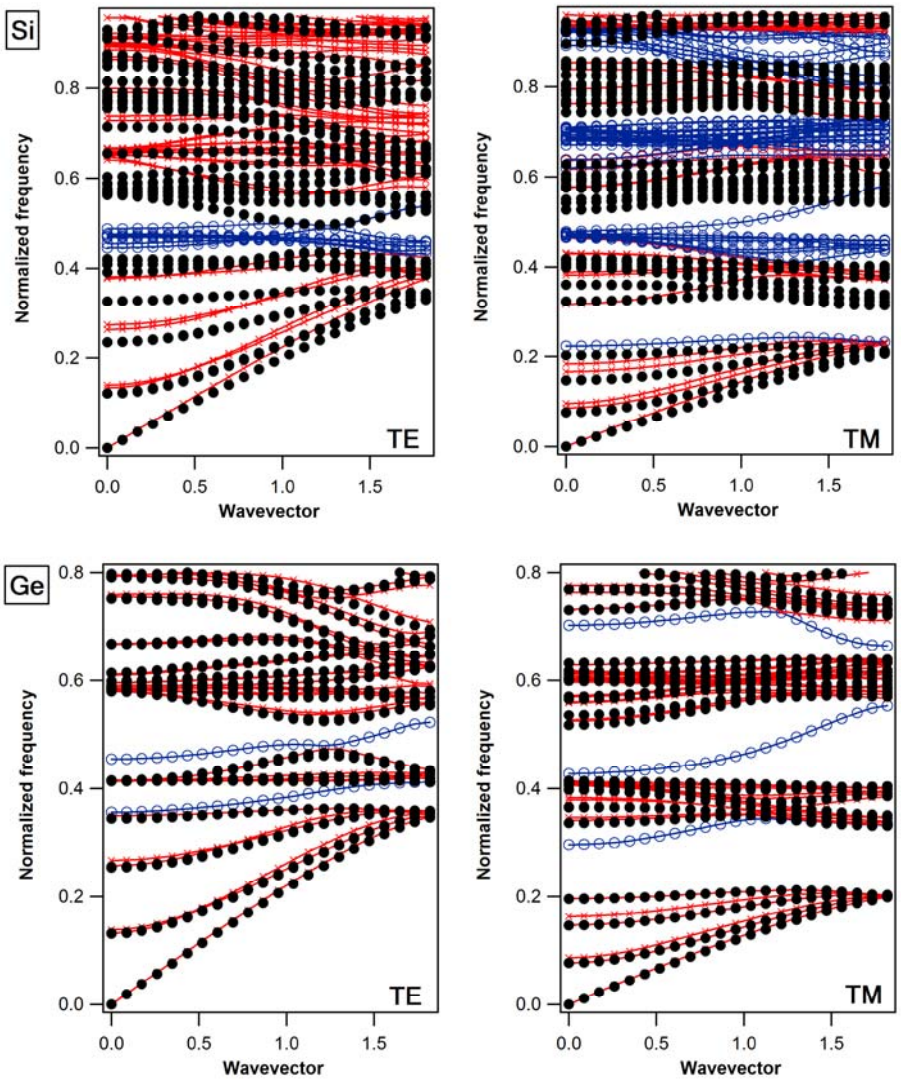

Fig. 4. Projected band-diagrams of W1 waveguide designed in a 2D PhC with hexagonal symmetry, using as materials Si and Ge and cylinder radius of r=0.25*a*. With black dots (●) are represented the bands of the pure crystal and with red lines (□), the ones of the defect. The blue lines (□), localized within the gap are associated with bound states supported by the defect.

The first striking difference that can be notices from the square lattice case is the appearance of a complete gap for both TE and TM modes in the 0.46-0.54 frequency interval for Ge, which supports rigorously a single mode and 0.44-0.55

frequency range for Si, which is featured by a multimode signature. We can speculate about the later one that besides the mode going "upwards" there are also two additional ones, one of them almost un-dispersing, behaving as the effective medium in which it travels is 0. A material with zero refractive index can be imagined as one in which light propagates accumulating any phase, spreading through the artificial medium as if the medium is completely missing in space. Such an optical nanostructure or metamaterial, with a zero index of refraction and fully controlled light dispersion has recently been engineered [23,29]. This is the case of the modes that can be guided infinitely long in the waveguide due to their vanishing group velocity.

Also, there are two TM-only gaps for each case, Si-PhC defect and for the Ge-PhC defect, and the previous discussion applies to the mode in the upper TM band with the mention that the variation of the supported mode changes suddenly, and this corresponds to the case of a negative effective refraction index. As a general remark about the case presented in Figure 4, we observe that the main difference between Ge and Si is the signature of a single guided mode for the material with higher refractive index, and an almost continuum of bands, corresponding to at least five bound modes for the case of Si. This observation could be useful depending on the kind of application desired: application based on single, well collimated modes are best suited in Ge materials, while those based on multimode devices are more efficiently realized using Si.

Now, returning to the case of guides designed in square-symmetry PhCs, Figures 5 present the projected band-structure of a periodic system with a cylinder radius r=0.3*a*. Neither this situation reveals any complete TE+TM gap, but only in this case a brief inspection is enough for concluding that both Si and Ge generated PhC are highly similar. It is worth mentioning that the TM gaps of the Ge PhC are approximately 10% wider than of the Si. This observation is useful for other kinds of defects or resonant cavities, with a pattern more complicated than W1, which can induce a more complicated band structure. In this case, at least in theory Ge seems more suitable, allowing a more flexible accommodation of defect-states, bound within the wider forbidden TM gap.

On the other hand, the upper band of Si PhC (B3), lying from 0.61 to 0.64 is featured by a bound state which is completely included in the TM gap and moreover, from $\mathbf{k}$=0.35(2π/a) to $\mathbf{k}$=0.5(2π/a), its dispersion mimics a material with negative effective refraction index since the frequency lowers as the wave vector values increases.

Its counterpart is presented in Fig. 6, where a hexagonal-based lattice structure is presented. Unlike the r=0.30*a* case, the projected band-diagram is not so rich in bound modes available for being guided and for further confinement. Both Si and Ge structures are featured by a central complete gap with comparable magnitudes, ranging in the 0.41-0.46 frequency window. Additionally, there are

three more TM gaps for both the Si and Ge structure which could presumably cover a wide branch of applications from microwave to near-IR and visible domains, again with the precondition that such defects are engineered so that their supported modes lie within those gaps.

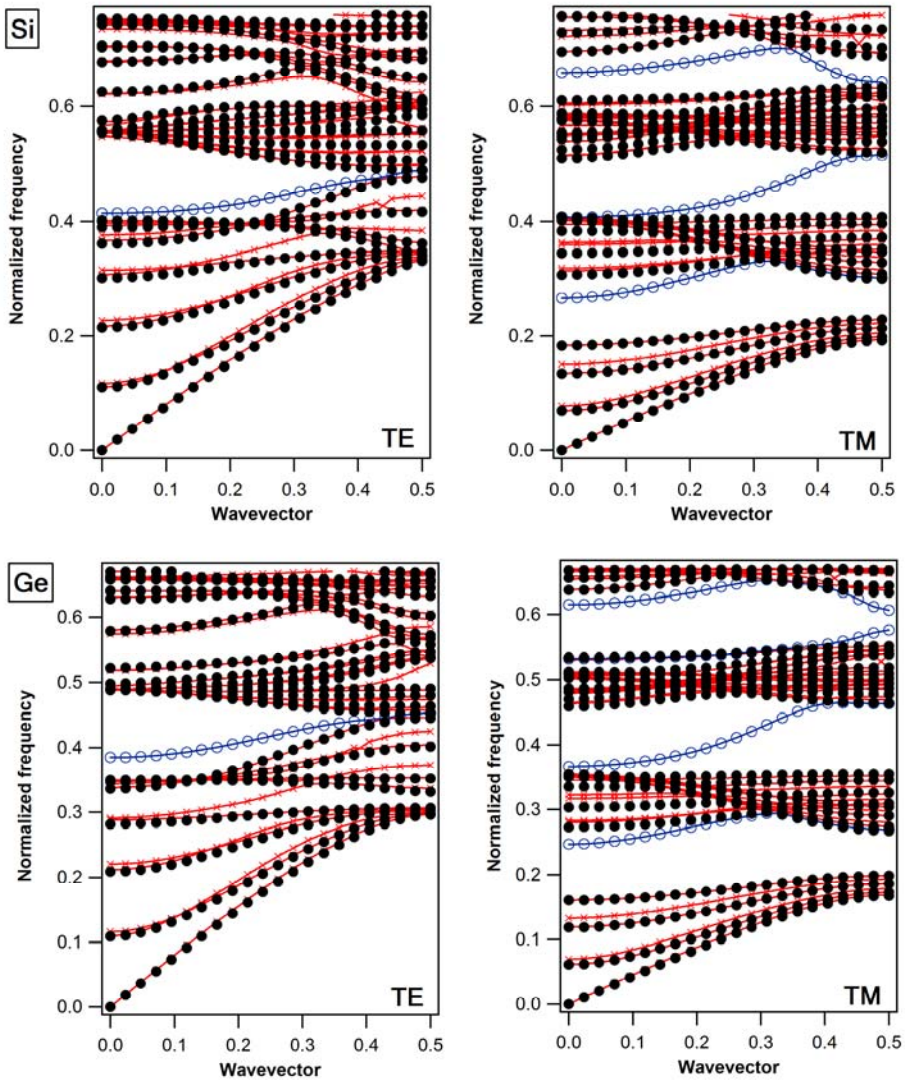

Fig. 5. Projected band-diagrams of W1 waveguide designed in a 2D PhC with square symmetry, using as materials Si and Ge and cylinder radius of r=0.3*a*. With black dots (●) are represented the bands of the pure crystal and with red lines (□), the ones of the defect. The blue lines (□), localized within the gap are associated with bound states supported by the defect.

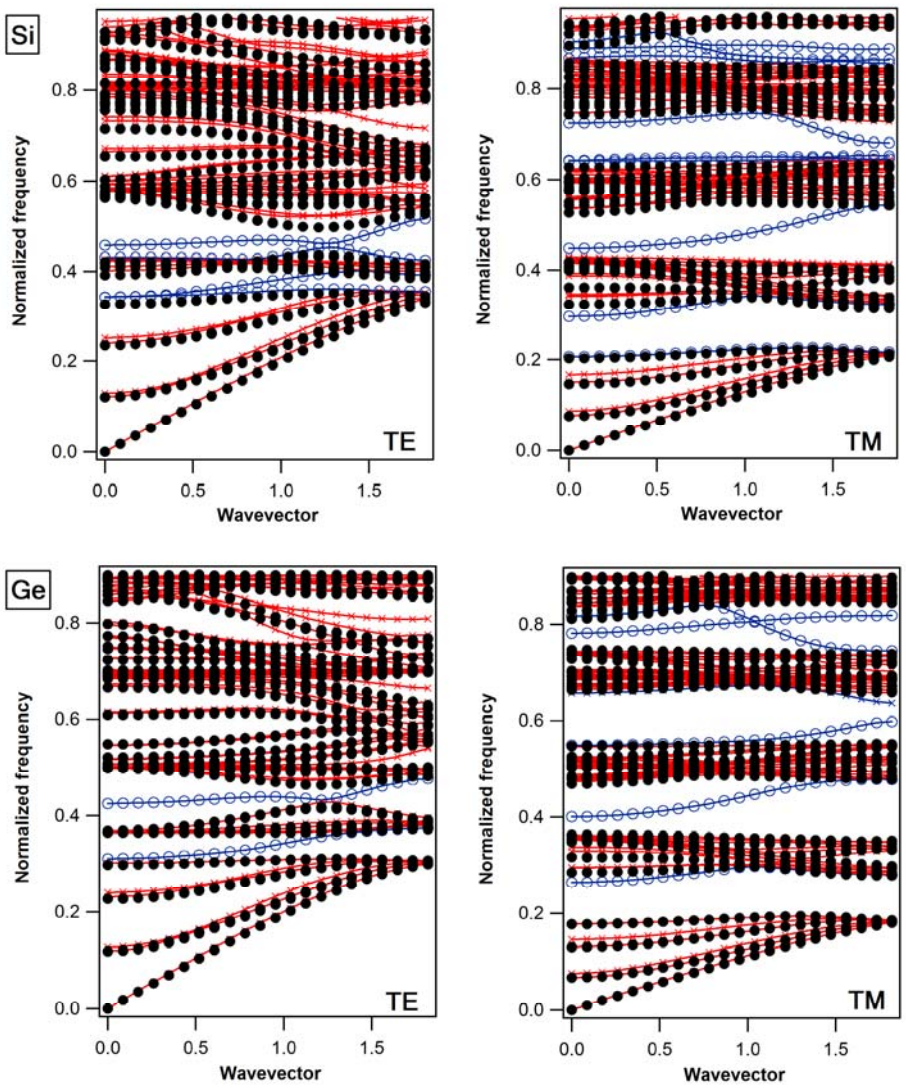

Fig. 6. Projected band-diagrams of W1 waveguide designed in a 2D PhC with hexagonal symmetry, using as materials Si and Ge and cylinder radius of r=0.3*a*. With black dots (●) are represented the bands of the pure crystal and with red lines (□), the ones of the defect. The blue lines (□), localized within the gap are associated with bound states supported by the defect.

Figs. 7 and 8 shows respectively the variation of the gaps, the number and the position of the defect states for linear defects designed in square lattice PhC and hexagonal one, when the radius of the elements is r=0.4*a*.

We can observe that increasing the dimension of the cylinders result in almost complete fading away of both the gaps and consequently of the bound states.

We see that as the cylinder radius increases, the magnitude of the gaps decreases. This fact can be understood based on the analogy with its "mirror"-case, when the periodicity is generated by piercing a material with high dielectric constant with holes infinitely high, filled with a low refraction index material (air for example). It is well known the inverse behavior of the gaps magnitude, compared with the dielectric cylinders situation: as the radius of the holes decreases from r~0.4a-0.45a, the gap diminishes and finally falls into a continuous structure of bands as the radius of the holes approaches values r<0.3a. The difference is that for the pierced infinite layer, the major photonic gaps are for the TE modes and only accidentally for TM ones. The appearance of TE modes in PhCs with a high filling fraction, where f is defined as the ratio between the volume of the high-index material and low index one is consistent with the general behavior of the electromagnetic waves at the interface with an infinite conductive material. The perpendicular magnetic component of the radiation field vanishes and the only surviving component being the TE one.

In order to evidence the ability of Ge-based waveguides designed in PhCs as alternative to Si, we theoretically calculated the modes of a set of coupled resonant cavities designed in a hexagonal lattice, as depicted in Figure 9. The radius of each element is r=0.3.

The modes represented correspond to two bound states, one located in the second TM band (see Fig. 6) and the second one within the upper TM band, which are highly confined within the cavities.

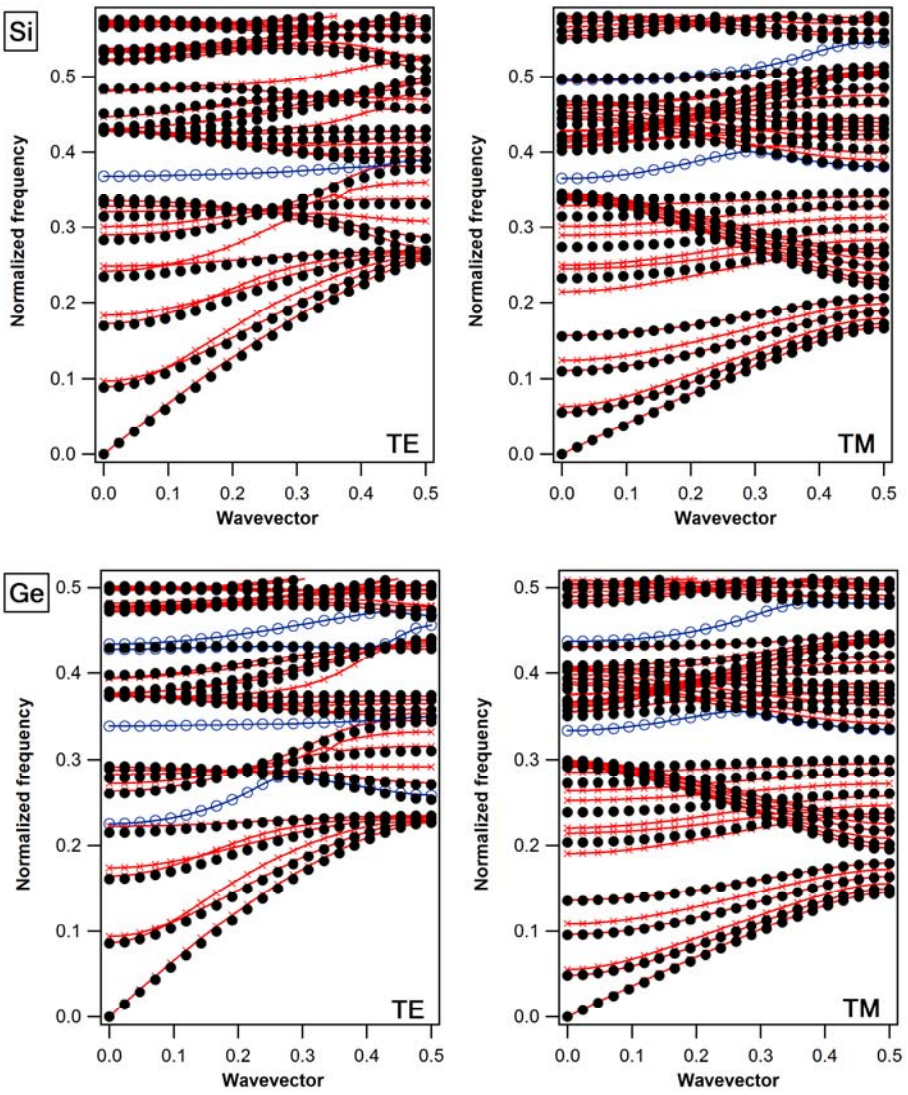

Fig. 7. Projected band-diagrams of W1 waveguide designed in a 2D PhC with square symmetry, using as materials Si and Ge and cylinder radius of r=0.4*a*. With black dots (●) are represented the bands of the pure crystal and with red lines (□), the ones of the defect. The blue lines (□), localized within the gap are associated with bound states supported by the defect.

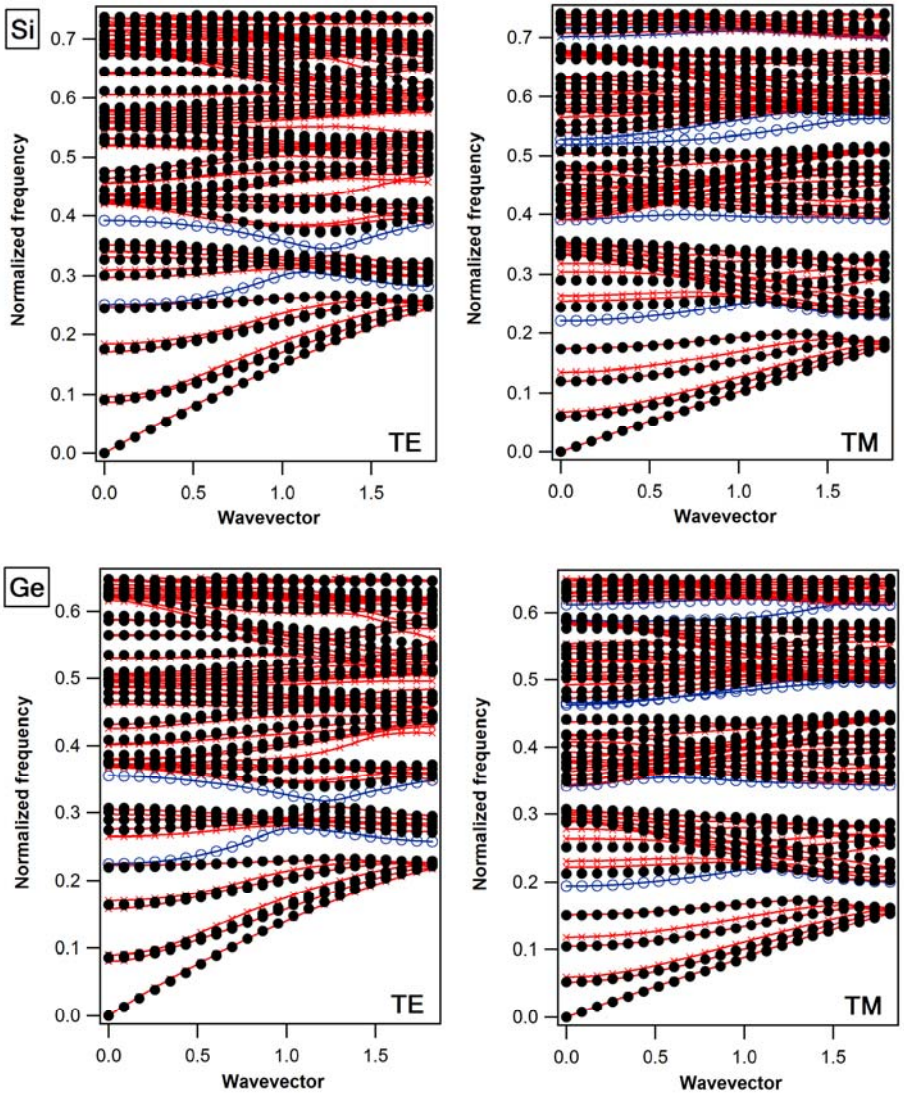

Fig. 8. Projected band-diagrams of W1 waveguide designed in a 2D PhC with hexagonal symmetry, using as materials Si and Ge and cylinder radius of r=0.4*a*. With black dots (●) are represented the bands of the pure crystal and with red lines (□), the ones of the defect. The blue lines (□), localized within the gap are associated with bound states supported by the defect.

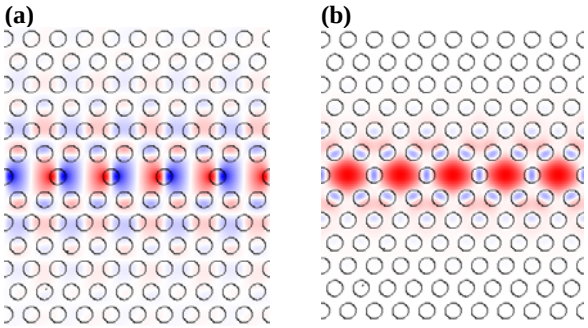

Fig. 9. Coupled resonant cavities operating at two different frequencies (0.43 and 0.78)

Fig. 10 illustrates the propagation of the field along a W1 waveguide in a PhC with square symmetry. We used a light source of 1.55µm choosing a rectangular shape of the incoming beam and a radius of the cylinders 0.3*a*. As a result we observed a well collimated field within y coordinates which propagates freely. There are also sketched the mode intensity profile along the waveguide and a 3D image of the radiation.

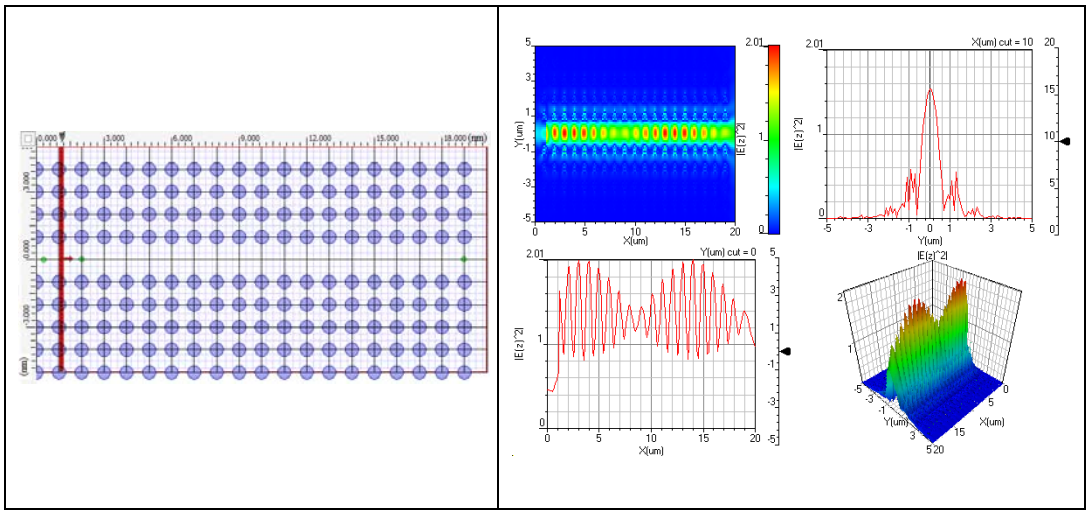

Fig. 10. On the left side is depicted a W1 waveguide; on the right side are illustrated a field map and other results of the simulation.

4. Conclusions

Concluding, we studied comparatively the PhCs with both square and hexagonal symmetry designed as cylinders with infinite height, with high refractive index separated by a low refractive index material (air), for applications

in guiding the radiation and confinement in resonant cavities. We varied the radius of the cylinders from r=0.25a to r=0.4a, studying the dispersion of the photonic bands in the Brillouin zone. The hexagonal structure is featured by complete gaps when the radius of cylinders is 0.25a or 0.3a, but they disappear when r=0.4a. This trend applies also in the case of square symmetry PhC, except that in this case, no complete gaps could be observed, the only significant downsize in the gap magnitude belongs to TM ones.

A design of a system with coupled cavities based on a hexagonal photonic crystal was also given, and further simulations within FDTD framework confirmed that when an incident radiation enters in a square waveguide with the frequency of a bound mode, it propagates without losses.

However it is still difficult to decide which material is best for this type of application, but we can assess that Ge can be used alternatively with Si in photonics, depending on the desired frequency range and on the application type.

Acknowledgement

This work was in part funded by the strategic project POSDRU/107/1.5/S/76909, inside POSDRU Romania 2007-2013 co-financed by the European Social Fund and by the UEFISCDI PCCE ID_76/2009 Project. The authors gratefully acknowledge the useful discussions and suggestions from Dr. Marius A. Husanu.

REFERENCES

[1] *Joannopoulos et. al.,* Photonic Crystals – Molding the Flow of Light, Princeton UniversityPress, 2008.

[2] *D.G. Popescu, P. Sterian*, "Nonlinear interaction modeling in photonic crystals", Annals of the Academy of Romanian Scientists, Series on Science and Technology of Information, **vol. 4**, issue 2, pp. 105-124, 2011.

[3] *D.G. Popescu,P. Sterian,* "FDTD analysis of photonic crystals with square and hexagonal symmetry", Journal of Advanced Research in Physics, vol. **2**, issue 2, pp. 1-5, 2011.

[4] *X.F. Yu, S.H. Fan*, "Bends and splitters for self-collimated beams in photonic crystals", Appl. Phys. Lett., vol. **83**, pp. 3251–3253, 2003.

[5] *Mortaza Noshad1, Amin Abbasi, Reza Ranjbar, Reza Kheradmand,* **"**Novel All-Optical Logic Gates Based on Photonic Crystal Structure", Journal of Physics: Conference Series, vol**. 350**, 012007, 2012.

[6] *R. F. Stancu, P. Sterian,* "Beam propagation and non-linear effects in photonic crystal optoelectronic devices", J. Optoel. Adv. Mat., Vol. **14,** Issue: 3-4, Pages: 371-375, 2012.

[7] *B. Lazar, P. Sterian*,"The multimode photonic crystal resonator and its application to unidirectional optical energy transfer", J. Optoel. Adv. Mat., Vol. **13,** Issue**:** 1-2, Pages: 32-40, 2011.

[8] *R. F. Stancu, P. Sterian,* "Photonic crystal optoelectronic devices and circuits for student training", Optoel. Adv. Mat., -Rapid Comm.Vol.**4,** Issue: 12, Pages: 2114-2117, 2010.

[9] *B. Lazar, P. Sterian,* "Band gaps in 2D photonic crystals with square symmetry", J. Optoel. Adv. Mat., Vol. **12,** Issue: 4, Pages: 810-817, 2010.

[10] *Kengo Nozaki et. al*, "Sub-femtojoule all-optical switching using a photonic-crystal nanocavity", Nature Photonics, vol**. 4**, pp. 477 – 483, 2010.
[11] *M. Djavid , F. Monifi, A. Ghaffari, M.S. Abrishamian*, "Heterostructure wavelength division demultiplexers using photonic crystal ring resonators", Optics Communications, vol. **281**, pp. 4028–4032, 2008.
[12] *D.G. Popescu, P. Sterian, Romeo Bercia, Cazimir Bostan*, "Second Harmonic Generation in Photonic Crystals: Numerical Simulation", J. Optoel. Adv. Mat., vol. **14**, pp. 356- 362, 2012.
[13]. *P.E. Sterian*, "Photonics", vol**.1**, (in Romanian), Printech Publishing House, Bucharest, 580 p., (ISBN 973-652-161-3), 2000.
[14] *G.A. Lungu, N.G. Apostol, L.E. Stoflea, R.M. Costescu, D.G. Popescu, C.M. Teodorescu*, "Room temperature ferromagnetic, anisotropic, germanium rich FeGe(001) alloys", Materials, vol. **6**(2), pp. 612-625, 2013.
[15] *D.G. Popescu, P. Sterian,* "Photonic Crystal Fiber Mode Characterization with Multipole Method", U.P.B. Sci. Bull., A Series, 75, pp. 205-215, 2013.
[16] *A. Taflove*, "Computational Electrodynamics: The Finite-Difference Time-Domain Method, Boston", Artech House Inc., 1995.
[17] *K.S. Yee*, "Numerical solution of initial boundary value problems involving Maxwell's equations in isotropic media", IEEE Trans. Antennas and Propagation, vol. **14**, pp. 302-307, 1966.
[18] *B. Lazar, P. Sterian,* "Photonic crystal band-stop filter with monomode resonator" J. Optoel. Adv. Mat., Vol.**12,** Issue: **1** Pages: 24-30, 2010.
[19] *B. Lazar, P. Sterian,* "Band gaps in 2d photonic crystals with hexagonal symmetry", J. Optoel. Adv. Mat., Vol. **10** Issue: 11, Pages: 2882-2889, 2008.
[20] *Colman, C. Husko, S. Combrie, I. Sagnes, C.W. Wong, A. De Rossi*, "Temporal solitons and pulse compression in photonic crystal waveguide", Nature Photonics, **vol. 4**, issue 12, pp. 862-868, 2010.
[21] *R.Courant, K. Friedrichs, H. Lewy*, "On the partial difference equations of mathematical physics", IBM J., vol. **11**, pp. 215-234, 1967.
[22] *J. P. Carini, J. T. Londergan, K. Mullen, D. P. Murdock*, "Bound states in waveguides and bent quantum wires. I. Applications to waveguide systems", Physical Review B, vol. **46**, pp. 4503, 1992.
[23] *J. P. Carini, J. T. Londergan, D. P. Murdock, D. Trinkle, C.S. Yung*, "Bound states and resonances in waveguides and quantum wires", Physical Review B**,** vol. **55**, pp. 9842, 1997.
[24] *A.M. Husanu,* "Electron-phonon interaction in zinc oxide. Plasmon-optical phonon coupled modes", Physica Status Solidi B, vol. **246**, pp. 87-91, 2009.
[25] *H. Wu, D. W. L. Sprung, J. Martorell*, "Electronic properties of quantum wire with arbitrary bending angle", Journal of Applied Physics, vol. **72**, p. 151, 1992.
[26] *K. Brunner*, "Si/Ge nanostructures", Rep. Prog. Phys., vol. **65**, pp. 27-72, 2002.
[27] *A. Sterian, P. Sterian,* "Mathematical Models of Dissipative Systems in Quantum Engineering**",** Mathematical Problems in Engineering, **vol**. 2012, Article ID 347674, 12 pages, doi:10.1155/2012/347674, 2012.
[28] *D.G. Popescu, M.A. Husanu,* "Au-Ge bonding on uniformly Au-covered Ge(001) surface", Phys. Status Solidi RRL, vol. **7**, pp. 274-277, 2013.
[29] *R. D. Meade, A. M. Rappe, K. D. Brommer, J. D. Joannopoulos*, "Accurate analysis of photonic band-gap materials", Physical Review B, vol. **48**, pp. 8434,1993.
[30] *O. Vakhnenko*, "Spectral and transport characteristics of an arbitrarily bent planar quantum electron guide", Physical Review B, vol. **52**, pp. 17386,1995.